

ACKNOWLEDGMENT

This work was supported by the Scientific and Technological Research Council of Turkey (TUBITAK) under Grant EEEAG-105E022.

REFERENCES

1. C. Karpuz and A. Görür, Quasi-static solutions of elliptical coplanar waveguides, *Microwave Opt Technol Lett* 20 (1999), 385–389.
2. N. Dib and A. Omar, Dispersion analysis of multilayer cylindrical transmission lines containing magnetized ferrite substrates, *IEEE Trans Microwave Theory Tech* 50 (2002), 1730–1736.
3. V. Akan and E. Yazgan, Quasi-static TEM characteristics of multilayer elliptical and cylindrical coplanar waveguides, *Microwave Opt Technol Lett* 42 (2004), 317–322.
4. B.N. Das and K.V.S.V.R. Prasad, Even- and odd-mode impedances of coupled elliptic arc strips, *IEEE Trans Microwave Theory Tech* MTT-32 (1984), 2689–2694.
5. M. Duyar, V. Akan, E. Yazgan, and M. Bayrak, Analyses of elliptical coplanar coupled waveguides and coplanar coupled waveguides with finite ground width, *IEEE Trans Microwave Theory Tech* 54 (2006), 1388–1395.
6. F. Medina and M. Horno, Spectral and variational analysis of generalized cylindrical elliptical strip and microstrip lines, *IEEE Trans Microwave Theory Tech* 38 (1990), 1287–1293.
7. D. Homentcovschi, G. Ghione, C. Naldi, and R. Oprea, Analytic determination of the capacitance matrix of planar or cylindrical multiconductor lines on multilayered substrates, *IEEE Trans Microwave Theory Tech* 43 (1995), 363–373.
8. G. Ghione and C.U. Naldi, Coplanar waveguides for MMIC Applications: Effect of upper shielding, conductor backing, finite extent ground planes, and line to line coupling, *IEEE Trans Microwave Theory Tech* MTT-35 (1987), 260–267.
9. K.K.M. Cheng, Analytical formula for calculating the coupling characteristics between parallel coplanar lines, *Electron Lett* 32 (1996), 1208–1209.
10. K.K.M. Cheng, Characteristic parameters of symmetrical triple coupled CPW lines, *Electron Lett* 33 (1997), 685–687.
11. K.-K.M. Cheng, Effect of conductor backing on the line-to-line coupling between parallel coplanar lines, *IEEE Trans Microwave Theory Tech* 45 (1997), 1132–1134.
12. K.-K. Cheng and I.D. Robertson, Quasi-TEM study of microshield lines with practical cavity sidewall profiles, *IEEE Trans Microwave Theory Tech* 43 (1995), 2689–2694.

© 2007 Wiley Periodicals, Inc.

CYLINDRICAL DOUBLE-RIDGED WAVEGUIDE AS A BASIC UNIT OF MICROWAVE HEATING APPLICATORS

Vyacheslav V. Komarov,¹ Yuriy N. Pchel'nikov,² and Vadim V. Yakovlev³

¹ Department of Radio Engineering, Saratov State Technical University, Saratov 410054, Russia

² SloWaveS, Inc., Cary, NC 27519

³ Department of Mathematical Sciences, Worcester Polytechnic Institute, Worcester, MA 01609

Received 28 November 2006

ABSTRACT: This paper deals with a circular double-ridged waveguide (CDRW) as a key element of traveling-wave systems for microwave thermal processing. Approximate formulas for estimation of basic characteristics of CDRW partially filled with dielectric are derived with the use of the equivalent circuit technique. For accurate analysis, 3D FDTD models are developed and used for computation of coupling, electric field, and dissipated power in a coaxially excited five-section CDRW applica-

tor with three spherical loads. © 2007 Wiley Periodicals, Inc. *Microwave Opt Technol Lett* 49: 1708–1713, 2007; Published online in Wiley InterScience (www.interscience.wiley.com). DOI 10.1002/mop.22539

Key words: cutoff frequency; dissipated power; electric field; equivalent circuit; capacitive gap; microwave heating; spherical load

1. INTRODUCTION

Well-known ridged and double-ridged waveguides along with quadruple-ridged [1], trapezoidal-ridged [2], ridge-through waveguides [3], waveguides with L-septa [4], and hourseshoe-shaped waveguides [5] are encountered in microwave devices where broadband operation is required. However, the longitudinal ridges also make a dramatic impact on the field: compared with a rectangular waveguide, the electric field in the area between the ridges is distributed relatively uniformly. The same can be observed in single-, double-, triple-, and quadruple-ridged circular guides [6, 7].

All these waveguide cross-sections constitute the group of transmission lines with the capacitive gap (CG) [8]. The advantages normally mentioned about them also include low wave impedance and smaller sizes at the given frequency in comparison with the related standard waveguides. The phenomenon of the electric field being primarily concentrated in the gap area and the magnetic field being pushed into the lateral troughs is another attractive feature of these cross-sections. It makes the field in the CG less sensitive to the electromagnetic parameters of the material placed there. This suggests that the CG structure may be advantageous in applications associated with microwave thermal processing of dielectrics [8]. Referring specifically to one of the waveguides in this group, a circular double-ridged waveguide (CDRW) [Fig. 1(a)], the load conveniently placed between the two ridges is subjected to more intense and efficient processing than in the corresponding circular applicator.

While several publications analyzed CG waveguides containing a dielectric in the gap [9–12], very few authors went in their analysis beyond eigen parameters (e.g. cutoff wavelengths and the wave impedance) and provided results for the field structure [1, 2, 11–13]. Furthermore, the principles of design of related applicators and particularly the techniques of their efficient excitation have received virtually no attention in literature. This explains why the CG systems have not yet found an appropriate use in microwave power engineering.

In this contribution, for the first time, we consider a CDRW as a basic unit of a traveling-wave applicator for thermal processing of dielectric objects in the gap. First, we present a simplified analysis (based on equivalent circuit approximation) of a CDRW whose CG contains a dielectric filling. Since major progress in studying this waveguide was held back by the complexity of its geometry, we suggest the design of a practical CDRW-based applicator to be essentially based on full-wave numerical modeling, allowing for adequate 3D analysis. We introduce a particular design and, instead of eigen fields, compute the electric field and dissipated power generated by coaxial excitation with a probe extended through the entire CG height. The presented modeling results are obtained for spherical loads with material parameters of an orange.

2. APPROXIMATE ANALYSIS

Microwave waveguide applicators may be designed in different ways—as (possibly, re-entrant) resonant cavities [14, 15], or (possibly, conveyorized) systems with a traveling wave [16].

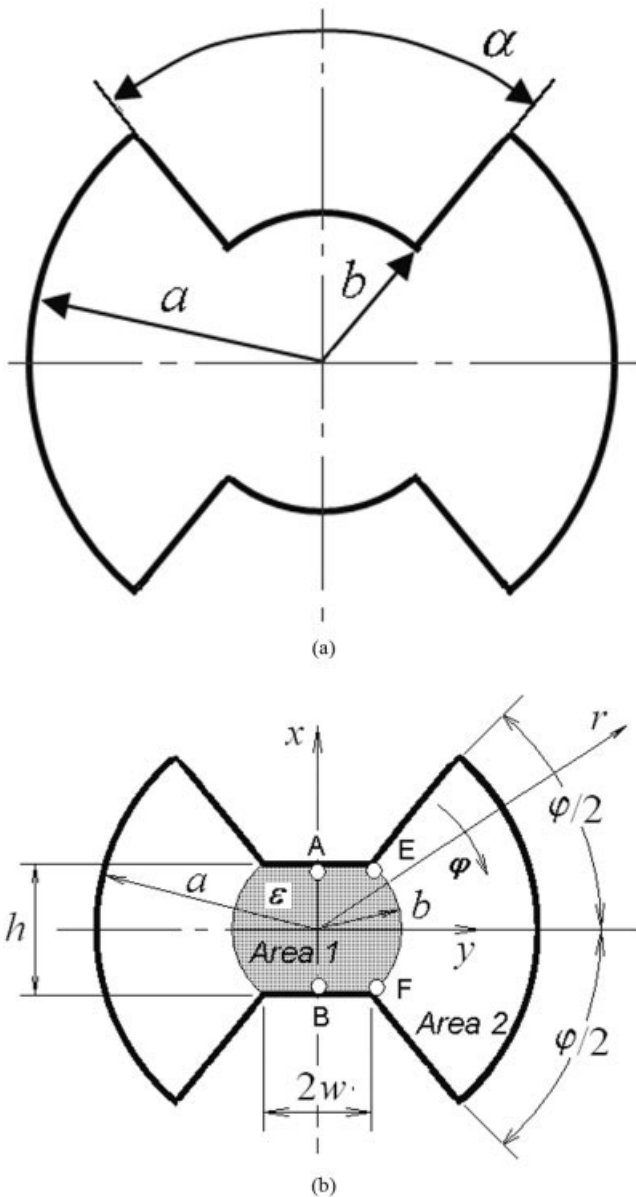


Figure 1 CDRW cross-section (a) and the cross-sectional geometry of the approximate analysis (b)

Some basic characterization of a partially filled CDRW and evaluation of applicability of this waveguide in specific microwave heating scenarios can be performed with the help of a simplified approximate analysis. Due to the spatial splitting of the electric and magnetic fields, the CDRW cross-section can be interpreted in terms of a corresponding LC-circuit. Approaches employing equivalent circuits for approximating parameters of complex waveguides are proved to be efficient and practical [11, 17, 18]. Here, we show that this technique can be used to estimate the wave impedance and the cutoff frequency of the CDRW with a dielectric in the CG.

Normally, the ridges inserted in the circular domain of a CDRW are assumed to be conically shaped; this is to avoid, in the framework of a rigorous analysis, mixed coordinate systems, which occur when rectangular ridges are utilized in a cylindrical waveguide [6]. However, an LC-formulation can avoid an excessive complication if we develop it for the cross-section shown in Figure 1(b) instead of working with a cylindrical CG. In this case,

we construct an equivalent circuit consisting of the inductance L_0 in the z -direction and the capacitance C_0 in the x -direction. It is assumed that C_0 is formed by C_t as the effective capacitance between the ridges and L_t as the inductance of the trough's walls (Fig. 2) so that $C_0 = C_t \left(1 - \frac{1}{\omega^2 L_t C_t} \right)$, where ω is the angular frequency. Then the phase factor β can be represented as

$$\beta^2 = k^2 - \Omega^2, \quad (1)$$

where $k = \omega \sqrt{\epsilon_0 \mu_0}$ is the wave number, ϵ_0 and μ_0 are permittivity and permeability of free space, and Ω is the transverse wave number:

$$\Omega^2 = \frac{\epsilon_0 \mu_0}{L_t C_t} \quad (2)$$

Using the LC-formulation for the wave impedance Z_0 [19], the latter then can be expressed in terms of C_t and L_t as

$$Z_0 = \frac{k}{\beta} \sqrt{\frac{L_t}{C_t}} \Omega \quad (3)$$

2.1. Large CG ($a/b > 2$)

In the symmetric half of the CDRW cross-section, the capacitance area of width w (Area 1) is filled with a dielectric with relative permittivity ϵ while the inductance area formed by the circular arcs of radii a and b (Area 2) is empty.

The electric field distribution in Area 1 is approximately the same as in the domain between the two ridges with the width $2w$; in Area 2 the field pattern is analogous to the field of the TE_{01} mode in the respective circular waveguide. Due to the field symmetry, the input impedance of Area 1 at the arc EF can be approximately represented by

$$Z_1 = -i \sqrt{\frac{\mu_0}{\epsilon_0 \epsilon}} h \cot \Omega_1 w \quad (4)$$

where $\Omega_1^2 = k^2 \epsilon - \beta^2$ is the transverse wave number of Area 1 and h is the CG height.

Using the expressions for the E_φ and H_z components of the TE_{01} mode in a circular waveguide, we get the input impedance of Area 2 at the arc EF in the form:

$$Z_2 = ib \varphi \sqrt{\frac{\mu_0}{\epsilon_0}} \text{Tn}(b\Omega_2, a\Omega_2) \quad (5)$$

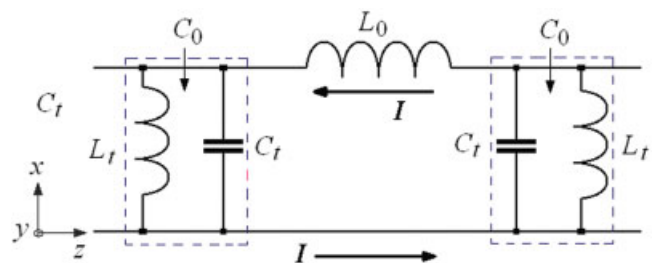


Figure 2 Equivalent circuit of the CDRW with a dielectric in the CG; I denotes the current in the longitudinal conductors of the circuit. [Color figure can be viewed in the online issue, which is available at www.interscience.wiley.com]

TABLE 1 Cutoff Frequencies (GHz) of the CDRW Dominant Mode for $\alpha = 10^\circ$ and $a = 92$ mm

	$(a - b)/a$	b (mm)			f_c	
[5]	0.2	73.6	0.917	0.873	0.829	0.754
[6]	0.3	64.4	0.925	0.877	0.830	0.763
Approximate technique	0.4	55.2	—	—	—	0.684
3D FDTD model	0.5	46	0.920	0.881	0.829	0.767

where

$$\text{Tn}(x, y) = \frac{J_1(x)Y_1(y) - J_1(y)Y_1(x)}{J_1(y)Y_0(x) - J_0(x)Y_1(y)}, \quad (6)$$

is the large radial tangent [20] expressed in terms of J_0 , J_1 , Y_0 , and Y_1 —that is, Bessel's functions of the first kind, of order 0 and 1, and of the second kind, of order 0 and 1, respectively, $\Omega_2^2 = k^2 - \beta^2$ is the transverse wave number of Area 2, and φ is the angular width of the CDRW cross-section [Fig. 1(b)].

Due to the equality of impedances on the boundary of Areas 1 and 2:

$$\frac{h}{\sqrt{\varepsilon}} \cot \Omega_1 w = b \varphi \frac{k}{\Omega_2} \text{Tn}(b\Omega_2, a\Omega_2) \quad (7)$$

Assuming that $\Omega_1 = k\sqrt{\varepsilon}$ and $\Omega_2 = k$, we determine a cutoff frequency of the dominant mode in the partially filled CDRW. With $h = b$ and $w = b$, Eq. (7) becomes

$$\frac{1}{\sqrt{\varepsilon}} \cot bk = \text{Tn}(bk, ak) \quad (8)$$

Solving (8) for bk , we calculate the cutoff frequency from the formula

$$f_c \approx \frac{c}{2\pi b} bk. \quad (9)$$

where c is the speed of light in free space.

2.2. Small CG ($a/b < 2$)

When the width of the gap w is relatively small, the LC formulation is expected to be more adequate if it is based on the equivalent static capacitance C_e considered between points A and B. Representing the CGs width in terms of the angular width of the ridges as $2w = b\alpha$ and using a formula for the capacitance formed by two relatively narrow plates [21], we obtain that

$$C_e \approx \varepsilon_0 \varepsilon \frac{\pi w}{\ln\left(\frac{2b}{w}\right)} \quad (10)$$

At the arc EF, the impedance of Area 1 can be written as

$$Z_1 = \frac{2}{i\omega C_e} = -i \frac{2 \ln\left(\frac{8}{\alpha}\right)}{\pi \varepsilon k} \sqrt{\frac{\mu_0}{\varepsilon_0}} \quad (11)$$

Equating the right-hand side of (11) with the right-hand side of (5) yields that for $\Omega_2 = k$

$$\frac{2 \ln\left(\frac{8}{\alpha}\right)}{\pi \varepsilon \varphi} = bk \text{Tn}(bk, ak) \quad (12)$$

Similarly, the cutoff frequency of the structure with the small CG can be calculated with (9) for bk obtained from (12).

The developed approach has been verified by computing a cutoff frequency determined by other analytical techniques. The accuracy of the suggested LC approximation naturally goes up with increasing values of permittivity of material in the CG. The result obtained with our approach for $\varepsilon = 1$ (see Table 1) differs by less than 10%. Since the Eqs. (13) and (26) are derived for Area 1 as a plane capacitor rather than a cylindrical one, we conclude that the accuracy of the described approximate analysis may be satisfactory for rough estimation of the basic characteristics of a partially filled CDRW.

Table 2 presents the cutoff frequencies of empty and partially filled CDRW computed with (8) and (9). A remarkable drop of f_c for higher ε is consistent with the results reported in [10, 11] and illustrates an attractive option of miniaturization of CDRW-based applicators.

3. ACCURATE NUMERICAL SIMULATION

While for CAD of practical microwave heating applicators eigen parameters are not instructive, results of 3D numerical analysis including the level of reflections from the system and patterns of the electric field and dissipated power are known to be valuable [22]; illustrations of the usefulness of this approach can be found in [23–26].

Later, we present the results of full-wave modeling of an empty CDRW and a realistic CDRW-based applicator with coaxial excitation. We employ 3D conformal FDTD models, which precisely reproduce the geometry, are completely parameterized, allow for easy changing of any geometrical parameters or inserting arbitrarily shaped materials with arbitrary losses, and for computing, in addition to eigen parameters, reflections/coupling in a frequency range as well as electromagnetic fields and dissipated power at a fixed frequency. Simulations were performed on a regular PC with the simulator QuickWave-3D (QW-3D) v. 5.0 [27].

3.1. CDRW

The model with a uniform mesh (maximum cell size: 5 mm) is used for computing cutoff frequencies. The figures in Table 1 are

TABLE 2 Cutoff Frequencies (GHz) of the CDRW Dominant Mode for $a = 92$ mm

a/b	ε	bk	f_c (GHz)
2	1	0.66	0.684
	4	0.36	0.374
	16	0.184	0.191
3	1	0.412	0.642
	4	0.22	0.342
	16	0.108	0.168

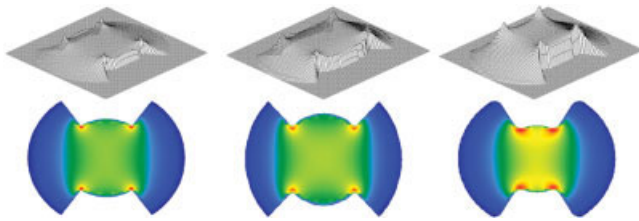


Figure 3 Electric field in a regular CDRW (a), CDRW with rounded ridges' edges (b), and CDRW with all sharp corners rounded (c) for $a = 92$ mm, $b = 52$ mm (a, b), 44 mm (c), $\alpha = 70^\circ$ (a), 90° (b), 50° (c) and the radius of the rounded corners $r = 5$ (b), 10 mm (c). [Color figure can be viewed in the online issue, which is available at www.interscience.wiley.com]

in a good agreement with the ones obtained by other methods. This validates our model and suggests that, with its appropriate upgrade for scenarios with dielectric fillings and some particular excitations, it should be able to provide quite accurate results and be responsible for CAD of the related applicators.

Placing the input (source) and output (load) ports on the opposite ends of the waveguide, we compute cross-sectional patterns of the electric field excited at 915 MHz (Fig. 3). Distribution of the field in the gap area is confirmed to be highly uniform, and the field magnitude naturally depends on the height of the gap. We also observe an increased concentration of the field near the ridges' corners. Though physically anticipated, this result has not been revealed in earlier computations of the electric field in other CG waveguides [1, 2, 11–13]—possibly due to the lack of spatial resolution of the related computational techniques. When the corners are rounded, this somewhat smooths the field's peaks out,

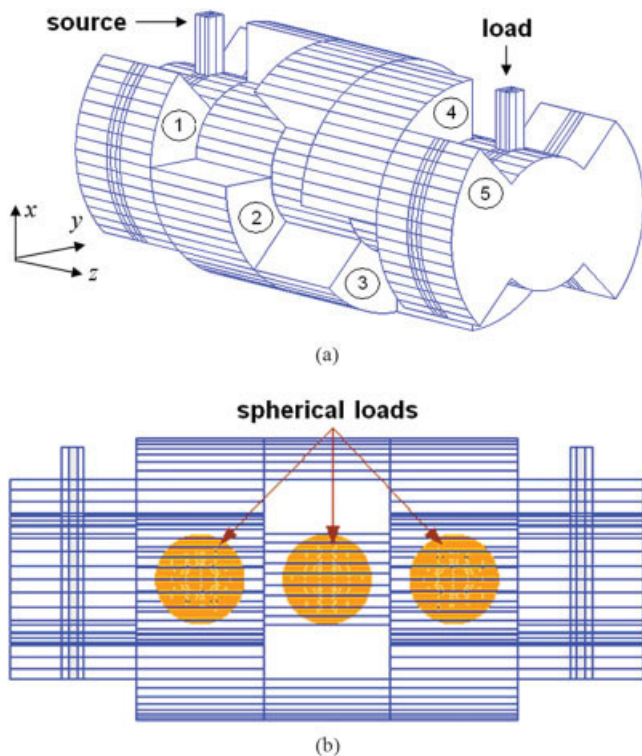


Figure 4 Coaxially excited five-sectional CDRW applicator with three processed spherical objects; section numbers are circled. [Color figure can be viewed in the online issue, which is available at www.interscience.wiley.com]

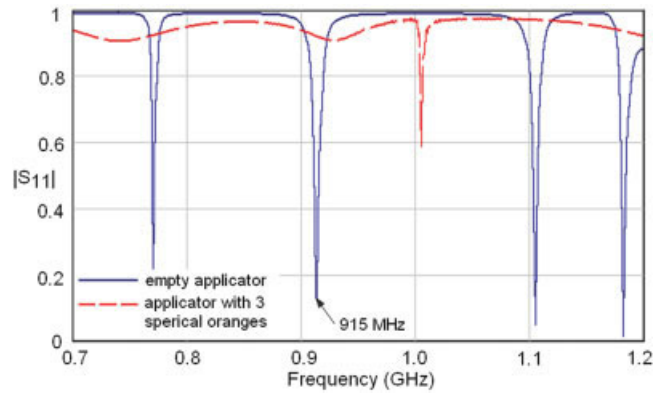


Figure 5 Resonance characteristic of the empty applicator (Fig. 4) with $a = 90$ mm, $b = 45$ mm, $\alpha = 80^\circ$, $r = 0$. [Color figure can be viewed in the online issue, which is available at www.interscience.wiley.com]

but does not eliminate them. As expected, rounding the troughs' corners produces virtually no effect on the field in the gap area.

3.2. CDRW-Based Applicator

Practical designs of CDRW-based microwave heating applicators are supposed to be application-dependent and, as such, may vary dramatically. In the present speculative study, we are concerned with CDRW properties, which may make the use of this waveguide in the corresponding applicators feasible as well as with corresponding modeling opportunities. The design proposed in this work as an example is based on the expectation that further

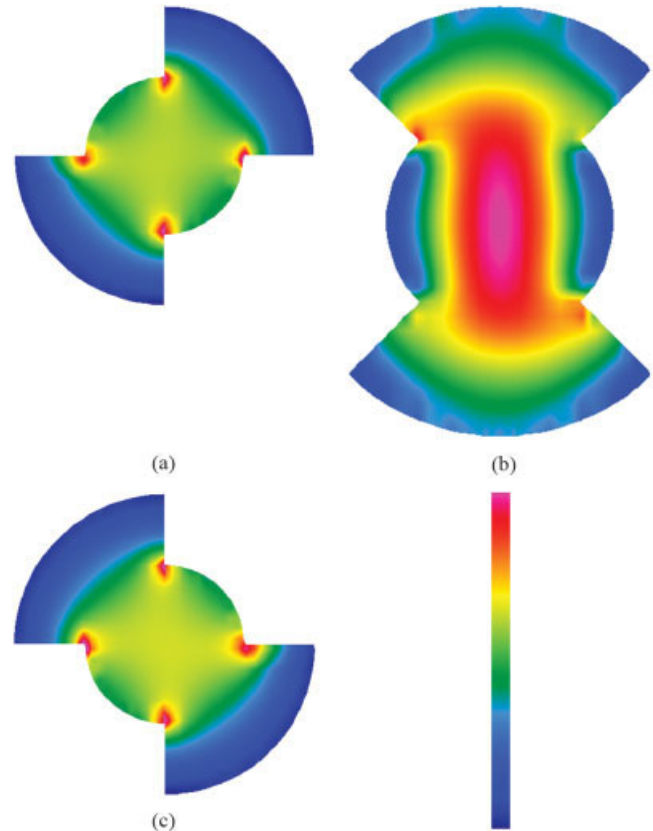


Figure 6 Electric field in the centers of the 2nd (a), 3rd (b), and 4th (c) sections of the empty applicator (Fig. 4). [Color figure can be viewed in the online issue, which is available at www.interscience.wiley.com]

improvement of uniformity of thermal processing of materials in the gap area can be achieved by rotating the plane of field polarization. Ideally, this can be implemented by continuous rotation of the ridges in the longitudinal direction. In practice, instead of a helical configuration, which may be difficult to manufacture, we suggest using a series of straightforward CDRW sections with the ridges revolving in the cross-sectional plane at some angle to each other. Also, we suppose that a dominant mode of the CDRW can be excited by the coaxial line with a probe positioned at $y = 0$ and extended along the x -axis through the entire height of the gap.

The modeling results below are obtained for the applicator (Fig. 4), which may find use in a postharvest thermal treatment of fruits [28]. It operates at 915 MHz and consists of five CDRW sections. The first and the fifth one are associated with the 50 Ω coaxial lines (outer diameter of 17.6 mm, centered on each ridge), and the others are loaded by three centered dielectric spheres of a 70 mm diameter with the material properties of a fresh orange (complex permittivity $\epsilon = 68.0 - i18.7$ [29]). A non-uniform mesh in the respective FDTD model also features 2-mm cells within the spheres and 1.5-mm cells around the coaxial lines.

First, placing the input and output ports in the coaxial lines, we find the applicator's geometry (parameters a , b , α) for which one of the resonances is situated at 915 MHz. A corresponding frequency response of the reflection coefficient S_{11} and the electric field patterns excited at 915 MHz in the cross-sectional planes are shown in Figures 5 and 6, respectively. The resonant characteristic is essentially destroyed in the presence of lossy loads (as indicated by the dashed curve in Fig. 5), so to get geometry of an efficient applicator, we look

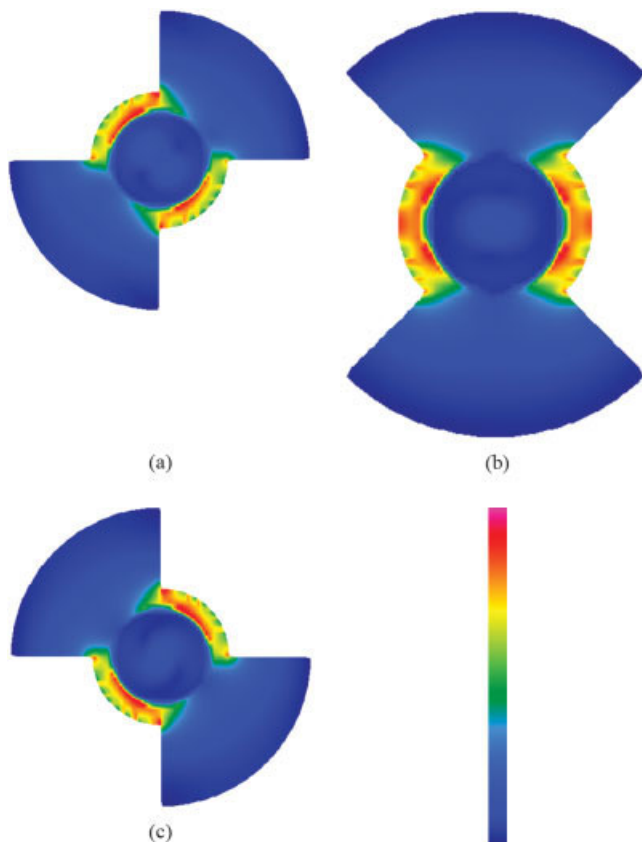


Figure 7 Electric field in the centers of the 2nd (a), 3rd (b), and 4th (c) sections of the applicator (Fig. 4) with spherical oranges of diameter 70 mm and $a = 111$ mm, $b = 51$ mm, $\alpha = 80^\circ$, $r = 0$. [Color figure can be viewed in the online issue, which is available at www.interscience.wiley.com]

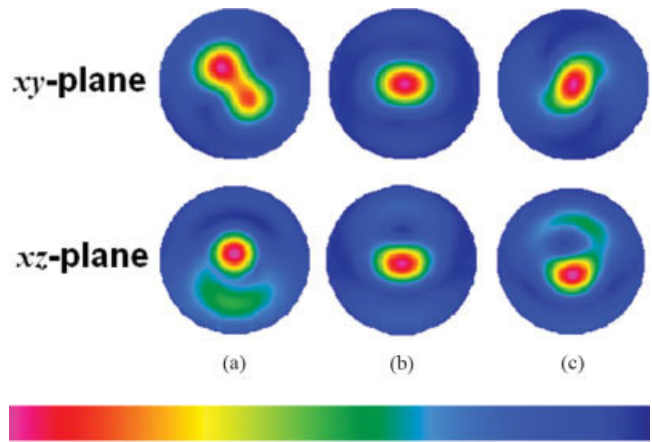


Figure 8 Dissipated power in two orthogonal planes through the spherical loads in the 2nd (a), 3rd (b), and 4th (c) sections of the applicator (Fig. 4) with $a = 111$ mm, $b = 51$ mm, $\alpha = 80^\circ$, $r = 0$. [Color figure can be viewed in the online issue, which is available at www.interscience.wiley.com]

for another set a , b , α corresponding to a minimum reflection from the system with spherical oranges. Corresponding field patterns in the xy -plane are given in Figure 7. Finally, Figure 8 shows the distributions of the dissipated power inside the processed oranges in two mutually orthogonal coordinate planes.

The presented results show a variety of options provided by full-wave 3D FDTD modeling for efficient CAD of applied microwave heating applicators constructed on the basis of CDRW and illustrate the advantages of this waveguide as a basic unit of microwave heating applicators.

4. CONCLUSION

In this paper, we have presented the arguments in favor of a CDRW as a key element of an efficient traveling-wave applicator, particularly suitable for processing of cylindrical and spherical objects. The techniques of both computer-free approximate analysis and accurate full-wave 3D computer modeling have been introduced for the CDRW and the five-sectional CDRW microwave heating applicator with three spherical loads. The FDTD models developed have been proved to be a convenient tool for computer-aided design of the CDRW-based applicators.

REFERENCES

1. W. Sun and C.A. Balanis, Analysis and design of quadruple-ridged waveguides, *IEEE Trans Microwave Theory Tech* MTT-42 (1994), 2201–2207.
2. M. Lu and P.J. Leonard, Design of trapezoidal-ridge waveguide by finite element method, *IEE Proc—Microwave Antennas Propag* 151 (2004), 205–211.
3. D. Guha and P.K. Saha, Some characteristics of ridge-through waveguide, *IEEE Trans Microwave Theory Tech* MTT-45 (1997), 449–453.
4. P.K. Saha and D. Guha, New broadband rectangular waveguide with L-shaped septa, *IEEE Trans Microwave Theory Tech* MTT-40 (1992), 777–781.
5. V.B. Katok, V.A. Kolomeytsev, and V.V. Yakovlev, Eigenvalues and structure of the electromagnetic fields of a horseshoe-shaped waveguide, *Radioelectron Commun Syst* 30 (1987), 15–20.
6. U. Balaji and R. Vahldieck, Radial mode matching analysis of ridged circular waveguides, *IEEE Trans Microwave Theory Tech* MTT-44 (1996), 1183–1186.
7. Q. Zhang, X. Zhou, and H. Yi, Propagation characteristic analysis of ridged circular waveguide using 2D finite difference frequency domain method, *Int J RF and Microwave CAE* 15 (2005), 264–271.

8. V.A. Kolomeyts and V.V. Yakovlev, Family of operating chambers for microwave thermal processing of dielectric materials, In: Proceedings of 29th IMPI Microwave Power Symposium, Chicago, IL, 1993, pp. 181–186.
9. P. Antony and F. Paolini, Heating of lossy films on a metal surface using a dielectric loaded T-septum waveguide, *J Microwave Power Electromagn Energy* 27 (1992), 112–117.
10. P.K. Saha and D. Guha, Characteristics of inhomogeneously filled double L-septa waveguide, *IEEE Trans Microwave Theory Tech MTT-40* (1992), 2050–2054.
11. V.V. Yakovlev, V.V. Komarov, and A.R. Zheleznyak, Analysis of horseshow-shaped waveguide with dielectric in capacitance gap, *IEEE Trans Magnetics MAG-2* (1993), 1616–1619.
12. M. Lu and M. Persson, Transmission characteristics of dielectric loaded double trapezoidal-ridge waveguide, *Microwave Opt Technol Lett* 49 (2007), 1–4.
13. D. Qiu, D.M. Klymyshyn, and P. Pramanick, Ridged waveguide structures with improved fundamental mode cutoff wavelength and bandwidth characteristics, *Int J RF and Microwave CAE* 12 (2002), 190–197.
14. Y. Kanai, T. Tsukamoto, M. Miyakawa, and T. Kashiwa, Resonant frequency analysis of re-entrant resonant cavity applicator by using FEM and FDTD method, *IEEE Trans Magnetics MAG-36* (2000), 1750–1753.
15. S. Kalhori, N. Elander, J. Svennebrink, and S. Stone-Elander, A re-entrant cavity for microwave-enhanced chemistry, *J Microwave Power Electromagn Energy* 38 (2003), 125–135.
16. A.C. Metaxas and R.J. Meredith, *Industrial microwave heating*, Peter Peregrinus, London, 1983.
17. T.S. Chen, Calculation of the parameters of ridge waveguide, *IRE Trans Microwave Theory Tech* 5 (1957), 12–17.
18. Yu.N. Pchel'nikov, E.V. Zyrova, and N.E. Ivanova, On a procedure for determining the parameters of equivalent circuit, *J Commun Technol Electron* 25 (1980), 90–95.
19. Yu.N. Pchel'nikov and A.A. Elizarov, Calculation of wave impedance of slow-wave systems at relative low frequencies, *J Commun Technol Electron* 40 (1996), 4–7.
20. N. Marcuvitz, *Waveguide handbook*, Dover, New York, 1965.
21. Yu.Ya. Iossel, E.S. Kochanov, and M.G. Strunskiy, Calculation of the electrical capacitance, *Emergoizdat*, Moscow, 1981 (in Russian).
22. V.V. Yakovlev, Examination of contemporary electromagnetic software capable of modeling problems of microwave heating, In: M. Willert-Porada (Ed.), *Advances in microwave and radio frequency processing*, Springer, New York, 2006, pp. 178–190.
23. E.E. Eves and V.V. Yakovlev, Analysis of operational regimes of a high power water load, *J Microwave Power Electromagn Energy* 37 (2002), 127–144.
24. J. Monzó-Cabrera, J. Escalante, A. Díaz-Morcillo, A. Martínez-González, and D. Sánchez-Hernández, Load matching in multimode microwave-heating applicators based on the use of dielectric-layer moulding with commercial materials, *Microwave Opt Technol Lett* 41 (2004), 414–417.
25. V.V. Komarov and V.V. Yakovlev, Coupling and power dissipation in a coaxially excited TM_{011} mode cylindrical applicator with a spherical load, *Microwave Opt Technol Lett* 48 (2006), 1104–1108.
26. V.V. Komarov and V.V. Yakovlev, CAD of single-mode elliptical applicators with coaxial excitation, In: Proceedings of 40th IMPI Microwave Power Symposium, Boston, MA, 2006, pp. 201–204.
27. QuickWave-3D™, QWED, Warsaw, Poland. Available at <http://www.qwed.com/pl/>.
28. J.N. Ikedia, J.D. Hansen, J. Tang, S.R. Drake, and S. Wang, Development of a saline water immersion technique with RF energy as a postharvest treatment against codling moth in cherries, *Postharvest Biol Tech* 24 (2002), 25–37.
29. S. Wang, J. Tang, J.A. Johnson, E. Mitchan, J.D. Hansen, G. Hallman, S.R. Drake, and Y. Wang, Dielectric properties of fruits and insects pests as related to RF and microwave treatments, *Biosyst Eng* 85 (2003), 201–212.

DESIGN, REALIZATION, AND TEST OF A 900 MHz CERAMIC OSCILLATOR

Stefano Pisa,¹ Emanuele Piuze,¹ Pasquale Tommasino,¹ Alessandro Trifiletti,¹ Alessandro Galli,¹ Giancarlo Giolo,² and Antonio Tafuto²

¹ Department of Electronic Engineering, "La Sapienza" University of Rome, Rome, Italy

² Microwave Department, Elettronica S.p.A., Rome, Italy

Received 6 December 2006

ABSTRACT: *The design of a 900 MHz ceramic oscillator, delivering a power of 10 dBm, has been carried out by using the negative-resistance condition. A new procedure based on the Nyquist criterion, implemented within microwave CADs has been used to test the onset of oscillations at the desired frequency and the presence of spurious oscillation. An excellent agreement between nonlinear simulations and measurements performed on a prototype has been observed.* © 2007 Wiley Periodicals, Inc. *Microwave Opt Technol Lett* 49: 1713–1717, 2007; Published online in Wiley InterScience (www.interscience.wiley.com). DOI 10.1002/mop.22528

Key words: oscillators; ceramic resonators; Nyquist criterion; hybrid RF circuits

1. INTRODUCTION

High-performance and low-cost oscillators are largely required due to the growth in the application of microwave and millimetre-wave systems. Each system requires oscillators with specific characteristics: e.g., when the oscillator operates as local reference for a receiver chain, a low phase noise is usually required; when the oscillator operates within a test circuit, the specifications on the output power and harmonics rejection are more stringent. Different configurations and design procedures have been developed in the last years to design oscillators at microwave frequencies [1–4]. A typical configuration consists of an active device in positive feedback coupled to resonators of different kinds (e.g., dielectric, coaxial, planar, etc.) to compose a hybrid low-cost oscillator. The hybrid configuration is still a challenging solution, if the production cost is a stringent demand and device size is not a constraint. For small-size applications, instead, an integrated solution is unavoidable. The design methodology of such hybrid devices is also a critical issue; as the oscillator operates in nonlinear regime, a nonlinear analysis is required to accurately simulate the oscillator performance. However, a straightforward design technique, based only on linear analysis and feasible to be implemented in linear simulators of commercially available CAD tools, would be helpful.

In this article, a design technique based on the linear analysis in frequency domain is presented and applied to the synthesis of a low-cost hybrid oscillator composed of a FET device and a coaxial resonator. The design criteria are presented in Section 2, and in Section 3 they are applied to the design of a 10 dBm oscillator at 0.9 GHz on RO4003 substrate. Finally, experimental test and comparison to simulated results are presented in Section 4.

2. METHODS

Microwave oscillators are generally realized by interfacing an active element with a resonator as shown in the block model of Figure 1.

The active element is generally realized by using a transistor with a series-series feedback applied to its source, thus obtaining a negative resistance behavior at the other two terminals. The